Journal of Chemical Neuroanatomy 131 (2023) 102288

Contents lists available at ScienceDirect

Journal of Chemical Neuroanatomy

journal homepage: www.elsevier.com/locate/jchemneu

A combined proteomics and bioinformatics analysis of ZNHIT1-interacting proteins reveals a significant enrichment in proteins associated with mitochondrial function

Jayanth Anantha [a], Fionnuala E. Wilson [a], Erin McCarthy [a], Noelia Morales-Prieto [a], Martina Mazzocchi [a], Louise M. Collins [a,b], Aideen M. Sullivan [a,b,c,*], Gerard W. O'Keeffe [a,b,c,*]

[a] Department of Anatomy & Neuroscience, University College Cork (UCC), Cork, Ireland
[b] Parkinson's Disease Research Cluster (PDRC), University College Cork, Cork, Ireland
[c] APC Microbiome Ireland, University College Cork, Cork, Ireland

ARTICLE INFO

Keywords:
ZNHIT1
Proteomics
Mitochondria
Parkinson's disease
Dopaminergic
ATP

ABSTRACT

Adenosine 5'-triphosphate (ATP) is the principal source of cellular energy, which is essential for neuronal health and maintenance. Parkinson's disease (PD) and other neurodegenerative disorders are characterised by impairments in mitochondrial function and reductions in cellular ATP levels. Thus there is a need to better understand the biology of intracellular regulators of ATP production, in order to inform the development of new neuroprotective therapies for diseases such as PD. One such regulator is Zinc finger HIT-domain containing protein 1 (ZNHIT1). ZNHIT1 is an evolutionarily-conserved component of a chromatin-remodelling complex, which has been recently shown to increase cellular ATP production in SH-SY5Y cells and to protect against impairments in mitochondrial function caused by alpha-synuclein, a protein which is integral to PD pathophysiology. This effect of ZNHIT1 on cellular ATP production is thought to be due to increased expression of genes associated with mitochondrial function, but it is also possible that ZNHIT1 regulates mitochondrial function by binding to mitochondrial proteins. To examine this question, we performed a combined proteomics and bioinformatics analysis to identify ZNHIT1-interacting proteins in SH-SY5Y cells. We report that ZNHIT1-interacting proteins are significantly enriched in multiple functional categories, including mitochondrial transport, ATP synthesis and ATP-dependent activity. Furthermore we also report that the correlation between ZNHIT1 and dopaminergic markers is reduced in the PD brain. These data suggest that the reported beneficial effects of ZNHIT1 on ATP production may be mediated, at least in part, by its direct interaction with mitochondrial proteins and suggest that potential alterations in ZNHIT1 in PD may contribute to the known impairments in ATP generation in midbrain dopaminergic neurons in PD.

1. Introduction

Adenosine 5'-triphosphate (ATP) is the principal source of energy in all cells, including neurons (Khakh and Burnstock, 2009). ATP, which is essential for neuronal health, is generated through oxidative phosphorylation by the electron transport chain in the inner mitochondrial membrane (Pathak et al., 2015). A growing body of evidence indicates that there is a decline in neuronal energy production during the ageing process, leading to a deficit in neuronal ATP generation (Blaszczyk, 2020). Furthermore, the age-related neurodegenerative disorder, Parkinson's disease (PD), is characterised by impairments in mitochondrial function and reduced cellular levels of ATP (Li et al., 2021; Moon and Paek, 2015). This is thought to contribute to the underlying pathology of PD, that is, progressive neurodegeneration of dopaminergic neurons

Abbreviations: ATP, Adenosine 5'-triphosphate; BSA, Bovine serum albumin; Co-IP, Co-immunoprecipitation; FDR, False discovery rate; FBS, Foetal bovine serum; GO, Gene ontology; HSP90B1, Heat Shock Protein 90 Beta Family Member 1; IP, Immunoprecipitation; LRRK2, Leucine rich repeat kinase 2; MPP^+, 1-methyl-4-phenylpyridinium; MPTP, 1-methyl-4-phenyl-1,2,3,6-tetrahydropyridine; PBS, Phosphate-buffered saline; PBS-T, 0.02% Triton X-100 in 10 mM PBS; PD, Parkinson's disease (PD); PPI, Protein–protein interaction; RESP18, Regulated endocrine specific protein 18; SLB, Sample loading buffer; SN, Substantia nigra; SRCAP, SNF2-related CBP activator protein; ZNHIT1, Zinc finger HIT-domain containing protein 1.

* Corresponding authors at: Department of Anatomy & Neuroscience, University College Cork (UCC), Cork, Ireland.
E-mail addresses: a.sullivan@ucc.ie (A.M. Sullivan), g.okeeffe@ucc.ie (G.W. O'Keeffe).

https://doi.org/10.1016/j.jchemneu.2023.102288
Received 14 December 2022; Received in revised form 5 May 2023; Accepted 10 May 2023
Available online 11 May 2023

which project from the substantia nigra (SN) to the striatum, and which are critical for movement control. This neurodegeneration results in reductions in striatal dopamine levels, leading to the cardinal motor impairments that are characteristic of this disease (Bloem et al., 2021; Goedert and Compston, 2018; Kordower et al., 2013). The underlying neuropathological feature of PD is the accumulation of intracellular aggregates of α-synuclein protein (Spillantini et al., 1998, 1997), which is known to cause mitochondrial dysfunction (Park et al., 2020; Wang et al., 2019).

The impact of reduction in cellular levels of ATP in PD on disease progression has been demonstrated by several studies. For example, treatment of PC12 cells or cultured embryonic mouse dopaminergic neurons, with agents that can maintain cellular ATP levels, has neuroprotective effects against ATP depletion and ER stress, as well as against cell death induced by the dopaminergic neurotoxin, 1-methyl-4-phenylpyridinium (MPP^+) (Nakano et al., 2017). These neuroprotective effects were also shown in the 1-methyl-4-phenyl-1,2,3,6-tetrahydropyridine (MPTP)-induced in vivo mouse model of PD (Nakano et al., 2017). Other studies have shown that treatment with terazosin, which increases brain levels of ATP, can slow or prevent dopaminergic neurodegeneration, partially restore striatal dopamine levels and improve motor function, in the MPTP mouse model of PD (Cai et al., 2019). Thus it is important to glean information about the biology of intracellular regulators of ATP production, in the context of new therapeutic approaches to neuroprotection in PD.

Zinc finger HIT-domain containing protein 1 (ZNHIT1) is an evolutionary-conserved component of the SNF2-related CBP activator protein (SRCAP) chromatin-remodelling complex, which acts to replaces histone H2A with the histone variant H2A.Z (Morrison and Shen, 2009). The H2A.Z variant controls nuclear-encoded mitochondrial gene expression which is essential for neuronal survival (Lowden et al., 2021). We have recently reported a link between ZNHIT1 and ATP production by showing that ZNHIT1 overexpression increases ATP production in SH-SY5Y cells and protects these cells against α-synuclein-induced impairments in mitochondrial function and neurite growth in a cellular model of relevance to PD (McCarthy et al., 2022). This provided proof for a functional role of ZNHIT1 in neuronal growth and in the regulation of cellular bioenergetic state, and suggested that ZNHIT1 may be a therapeutic target for PD. Moreover, we have also shown that *ZNHIT1*-co-expressed genes in the human SN were found to be significantly enriched in genes associated with the multiple gene ontologies that are linked to mitochondrial function (McCarthy et al., 2022). In support of this, the SRCAP chromatin-remodelling complex (of which ZNHIT1 is a key component) has been shown to promote oxidative metabolism during prenatal development of the heart (Xu et al., 2021a). These data show that ZNHIT1 plays a critical role in promoting mitochondrial function and ATP production. Although the effect of ZNHIT1 on cellular ATP production is thought to be due to increased expression of genes associated with mitochondrial function (Xu et al., 2021a), it is also possible that the effects of ZNHIT1 are mediated through other non-canonical pathways, such as binding of mitochondrial proteins, as has been shown for other nuclear proteins (Lindenboim et al., 2011). However there is limited information on ZNHIT1 expression in the human brain and it is important to investigate this.

In the current study, we analysed *ZNHIT1* expression in the human brain and performed ZNHIT1 immunoprecipitation followed by untargeted proteomics to identify ZNHIT1-interacting proteins in SH-SY5Y cells, which are commonly used to model dopaminergic neurons in the context of PD research. This analysis of the ZNHIT1-interacting proteins revealed a significant enrichment in proteins associated with mitochondrial function and ATP production. This suggests that the reported effects of ZNHIT1 on ATP production (McCarthy et al., 2022; Xu et al., 2021a) may be mediated, at least in part, by its direct interaction with mitochondrial proteins. Furthermore, we also show a loss of the co-expression of ZNHIT1 with markers of dopaminergic neurons at the transcript and protein level in the SN in PD.

2. Methods

2.1. Gene and protein expression analysis of human brain

Gene expression data on *ZNHIT1* expression in healthy control brains was generated from the GSE:60863 dataset from UK Brain Expression Consortium (Ramasamy et al., 2014a). This contains gene expression data on multiple regions of the human brain, using post-mortem brain samples obtained from 134 Caucasian neuropathologically and neurologically normal individuals. Gene co-expression data was generated from the GSE49036 dataset, which consists of gene expression data from age- and gender-matched control and PD post-mortem SN samples (Dijkstra et al., 2015). Gene expression and co-expression analyses were performed using the R2 Genomics Analysis and Visualization Platform (https://hgserver1.amc.nl/cgi-bin/r2/main.cgi). Data on ZNHIT1 gene and protein expression in the human brain was obtained from the Human Protein Atlas (Version 21.0) (https://www.proteinatlas.org) (Uhlen et al., 2015). Image credits: Human Protein Atlas. The image of ZNHIT1 staining and its intensity in the human cerebral cortex can be found here: v21.proteinatlas.org/ENSG00000106400-ZNHIT1/tissue/-cerebral+cortex#img. The image of HSP90B1staining and its intensity in the human cerebral cortex can be found here: v21.proteinatlas.org/ENSG00000166598-HSP90B1/tissue/cerebral+cortex#img.

2.2. Cell culture and transfection

SH-SY5Y cells were grown in a humidified incubator at 37 °C with 5% CO_2 in medium consisting of DMEM-high glucose, supplemented with 10% (v/v) foetal bovine serum (FBS), 1% (v/v) L-glutamine, 1% (v/v) penicillin/streptomycin, 1% (v/v) non-essential amino acids and 1% (v/v) sodium pyruvate (all from Sigma). For transfection experiments, cells were plated at a density of 2.5–3 × 10^6 cells per well of 6-well plate and grown for 16 h prior to transfection, which was performed with TransIT-X2® reagent following the manufacturer's guidelines. In brief, each well was transfected with 2 μg of a plasmid coding human ZNHIT1 with an N-terminal flag tag (Flag-ZNHIT1) (a gift from Joan Conaway & Ronald Conaway; Addgene plasmid #15332; http://n2t.net/addgene:15332). Cells were allowed to grow for an additional 24 h before immunoprecipitation (IP) was carried out.

2.3. Western blotting and Immunoprecipitation

For IP, growth medium was removed and cells were gently washed two times with ice-cold 1xPBS supplemented with a cocktail of protease inhibitors from Roche Molecular Biochemicals (Cat no. 11836170001). Cells were then lysed in 500 μl of ice-cold co-immunoprecipitation (Co-IP) buffer containing 50 mM HEPES, 150 mM NaCl, 1 mM EDTA, 0.1% (v/v) Nonidet P-40, 1 mM sodium orthovanadate, 1 mM sodium fluoride and the Roche protease inhibitor cocktail. Lysates were then centrifuged at 18,000 g (12000 RPM) at 4 °C for 20 min. To confirm protein expression, lysates were then mixed with 1 × sample loading buffer containing (5xSLB: 70 ml glycerol, 30 ml ddH2O, 2.5 g of SDS, 0.606 g of tris base with 5–6% β-mercaptoethanol) and were resolved on a 10% SDS-PAGE gel, transferred to a PVDF membrane, which was blocked in a blocking buffer containing 5% BSA in 10 mM PBS/TBS with 0.1% Tween20 for 2 h at room temperature. Membranes were washed three times with washing buffer containing 10 mM PBS with 0.1% Tween20. Following this, the membranes were incubated in either anti-GAPDH (SCBT: SC-47724, 1:1000) or anti-FLAG (Sigma: A2220, 1:1000) and incubated for 12–16 h at 4 °C. Following this, the blots were washed three times with washing buffer. The blots were then labelled with secondary antibodies in blocking buffer using the following HRP-conjugated secondary antibodies: anti-mouse 1:10,000 (ThermoFisher: Cat No. A27025) or anti-rabbit 1:2000 (ThermoFisher: Cat No. 31460).

To perform the IP, lysates were precleared for 2 h at room temperature on an upright tube rotor with 25 μl of recombinant protein G-

Sepharose beads (Invitrogen Cat no. 101242) pre-blocked with BSA. The beads were precipitated by centrifugation at 1000 g (3000RPM) for 5 min at 4 °C, then the supernatant was transferred into a fresh tube. The beads from the precleared lysates (designated as control beads) were then used as control beads to identify proteins that bind to the beads themselves. 5 μg of anti-Flag antibody (Sigma Cat no. A2220) was added to the supernatant and samples were incubated at 4 °C for 1 h on an upright tube rotor. 25 μl of pre-blocked recombinant protein G-Sepharose beads were then added, and incubated overnight on an upright tube rotor at 4 °C. Following this, beads were precipitated by centrifugation at 1000 g (3000RPM) for 5 min at 4 °C. Following this, the beads were washed in a wash buffer containing 50 mM HEPES, 150 mM NaCl, 1 mM EDTA, 0.1% (v/v) (IGEPAL) Nonidet P-40, 1 mM sodium orthovanadate, 1 mM sodium fluoride and cocktail protease inhibitors, and then centrifuged at 1000 x g (3000 RPM) for 5 min at 4 °C, this was repeated three times to ensure removal of any unbound proteins from the beads. After the third wash, the wash buffer was removed and 50 μl of Co-IP lysis buffer was added. Following this, 1x sample loading buffer (5 x sample loading buffer containing 70 ml glycerol 30 ml water with 0.2 g of bromophenol blue, 2.5 g sodium dodecyl sulphate, 0.606 g of Tris base with 5–6% v/v β-mercaptoethanol) was added, and the samples were boiled at 95 °C for 5 min. The control beads from the preclearing step were processed in the same way. The boiled IP samples and control samples were resolved on an 10% SDS-PAGE gel and once the dye front had migrated to 2 cm of the resolving gel, the electrophoresis was stopped, the gel lanes were excised using a sterile surgical blade and stored in sterile distilled deionized water for label-free mass spectrometry, following confirmation of pulldown using western blotting as described above.

2.4. Label-free mass spectrometry

The excised gel lanes from the immunoprecipitation were shipped to the Centre of Excellence for Mass Spectrometry in King's College London (London, UK) for analysis. Proteins were extracted from the excised gel lanes, the proteins were subjected to digestion with trypsin, then passed through a U3000 UHPLC Nano LC system for chromatography. Peptides were resolved using a three-step linear gradient consisting of 80% acetonitrile in 0.1% formic acid. The peptide elution was performed at a flow rate of 250 nl/min over 60 min. Electrospray ionisation was performed on an Orbitrap Fusion Lumos system (ThermoFisherScientific, UK) with an Xcalibur v4.3. The Orbitrap method was set to a 3-s time cycle between a full MS scan and an MS/MS fragmentation. The acquired raw mass spectrometry data were analysed using Proteome Discoverer v2.5 (ThermoScientific) and the peptide search was performed using Mascot and Sequest search engines on the Uniprot Human Taxonomy databases (50,351 entries), with the search stringency fixed at a 1% false discovery rate. From the resulting data, proteins that uniquely bind to ZNHIT1 were obtained by excluding proteins that bound to the Control beads from the preclear step of the immunoprecipitation and excluding any immunoglobulins used in the IP.

2.5. Immunocytochemistry

For immunocytochemistry, the media was removed and the cells were washed in 10 mM phosphate-buffered saline (PBS) and then fixed by immersion in 4% paraformaldehyde for 25 mins at room temperature. Following removal of the fixative, the cells were washed in three times for 5 min per wash in 0.02% Triton X-100 in 10 mM PBS (PBS-T). The cells were then incubated in 5% bovine serum albumin (BSA) in 10 mM PBS-T for 1 h at room temperature to block non-specific binding before they were incubated in primary antibody against ZNHIT1 (Thermo Fisher # PA5–53,903; 1:500) or FLAG (Sigma # A2220; 1:200), diluted in 1% BSA in 10 mM PBS at 4 °C for 16 h. Following three 5-min washes in 10 mM PBS-T, cells were incubated in 594-conjugated Alexa Fluor® secondary antibody (Invitrogen; 1:500 A11005 or A11012) in 1% BSA in 10 mM PBS, overnight at 4 °C, wash three times for 5 mins per wash in PBS-T, before they were imaged using an Olympus IX71 inverted microscope.

2.6. Immunohistochemistry on human brain samples

Immunohistochemical staining was performed on formalin-fixed paraffin-embedded coronal sections through the human midbrain from PD cases and healthy age-matched controls. The tissue and associated clinical and neuropathological data were supplied, with full ethical approval, by Parkinson's UK Brain Bank at Imperial College London, funded by Parkinson's UK, a charity registered in England and Wales (258197) and in Scotland (SC037554). Sections were dewaxed in Citroclear, rehydrated through a descending ethanol gradient (100%, 90%, 70%), then an antigen retrieval step was performed by incubation in 0.01 M sodium citrate buffer solution, pH 6.4, for 10 min at 90 °C. Sections were washed three times for 5 min in tris-buffered saline containing 0.02% Triton-X100. Non-specific staining was blocked by incubation in 10% goat serum diluted in 1.2% tris-buffered saline (TBS) for 1 hr. Sections were incubated in a solution of primary antibody in TBS containing 1% goat serum for 48 h at 4 °C. The following primary antibodies were used for immunofluorescent double-labelling; tyrosine hydroxylase (TH; 1:500; Merk Millipore; AB318) and ZNHIT1 (1:500; Thermofisher; PA5–53903). Following primary antibody incubation, sections were washed three times for 5 min in TBS, then incubated in solution of secondary antibody in 1% goat serum in TBS overnight at room temperature. For fluorescence staining, Alexa Fluor 488- or 594-conjugated secondary antibodies were used (1:500; Invitrogen). Sections were washed three times in TBS and nuclei were stained by incubation in DAPI (Sigma; 1:3000) solution for 5 min in the dark, followed by three TBS washes, then cover-slipped using fluorescent mounting media (Dako Diagnostics). Images were taken using an Olympus BX53 Upright Microscope.

2.7. Bioinformatics analysis

The list of proteins that were identified as interacting partners of ZNHIT1 from the proteomics experiment was used to generate a protein-protein interaction network using the STRING platform. Gene ontology (GO) enrichment analysis was performed using Panther (http://pantherdb.org; Version 17.0). An enrichment was deemed significant at a false discovery rate (FDR) adjusted p value of ($p < 0.05$).

3. Results

3.1. Expression and cellular localisation of ZNHIT1 in the adult human brain

We first investigated the expression of ZNHIT1 transcripts in the adult human brain, using available gene expression data (Gene expression Omnibus: GSE60863; (Ramasamy et al., 2014b)) for multiple regions of the adult human brain from neuropathologically and neurologically normal individuals. This analysis showed that the highest levels of *ZNHIT1* expression were found in the SN (mean log2 expression = 7.60 ± 0.026), followed by the putamen (mean log2 expression = 7.47 ± 0.017), with the lowest levels of *ZNHIT1* in the cerebellar cortex (mean log2 expression = 6.72 ± 0.026) (Fig. 1A). We next interrogated ZNHIT1 expression at the protein level using the Human Protein Atlas, which revealed that ZNHIT1 was strongly expressed in neuronal cells (Fig. 1B, C). This also revealed that, in addition to the expected strong expression in the nucleus, ZNHIT1 was also expressed, albeit at lower levels, in the cytoplasm and neurites of neurons (Fig. 1C, D). Given these findings, we next aimed to identify ZNHIT1-interacting proteins in a cellular model using immunoprecipitation of ZNHIT1, followed by label-free mass spectrometry.

A

Brain region	sample *n*	Log_2 ZNHIT1
Cerebellar cortex	*n* = 130	6.72 ± 0.023
Frontal cortex	*n* = 127	7.26 ± 0.018
Hippocampus	*n* = 122	7.38 ± 0.021
Occipital cortex	*n* = 129	7.19 ± 0.019
Putamen	*n* = 129	7.47 ± 0.017
Substantia nigra	*n* = 101	7.60 ± 0.026
Temporal cortex	*n* = 119	7.32 ± 0.015

C

Cell-type	Staining	Intensity
Neuronal cells	High	Strong
Glial cells	Low	Weak
Endothelial cells	Medium	Moderate
Neuropil	Low	Weak

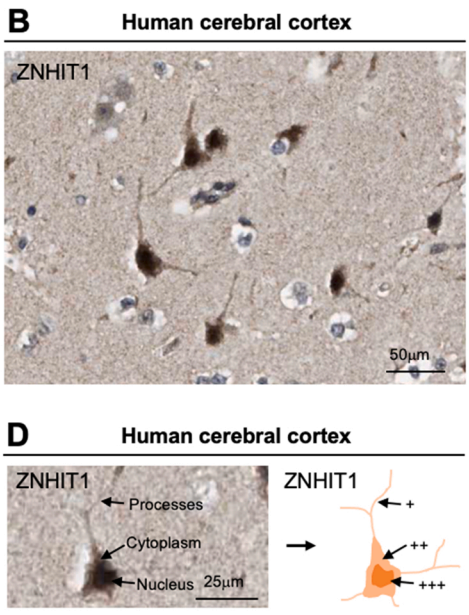

Fig. 1. Expression and cellular localisation of ZNHIT1 in the adult human brain.
(A) Table showing the mean ± SEM of log2 expression values for *ZNHIT1* in seven distinct regions of the human brain. Raw data was obtained from the Gene Expression Omnibus GSE60863 and analysed using the R2: Genomics analysis and visualisation platform (https://hgserver1.amc.nl/cgi-bin/r2/main.cgi). (B) Image showing ZNHIT1 expression in the human cerebral cortex. (C) Table showing quantification of ZNHIT1 staining in different cell types in the human cerebral cortex. (D) Image and tracing of a single neuron showing relative ZNHIT1 staining intensity in different compartments of a neuron in the human cerebral cortex (+++ = high, ++ = moderate, + = low). Image credits: Human Protein Atlas v. The image of ZNHIT1 staining and the accompanying data on the quantification of ZNHIT1 staining intensity in the human cerebral cortex can be found here: v21.proteinatlas.org/ENSG00000106400-ZNHIT1/tissue/cerebral+cortex#img. Scale bar in (B) = 50 μm and in (D) = 25 μm.

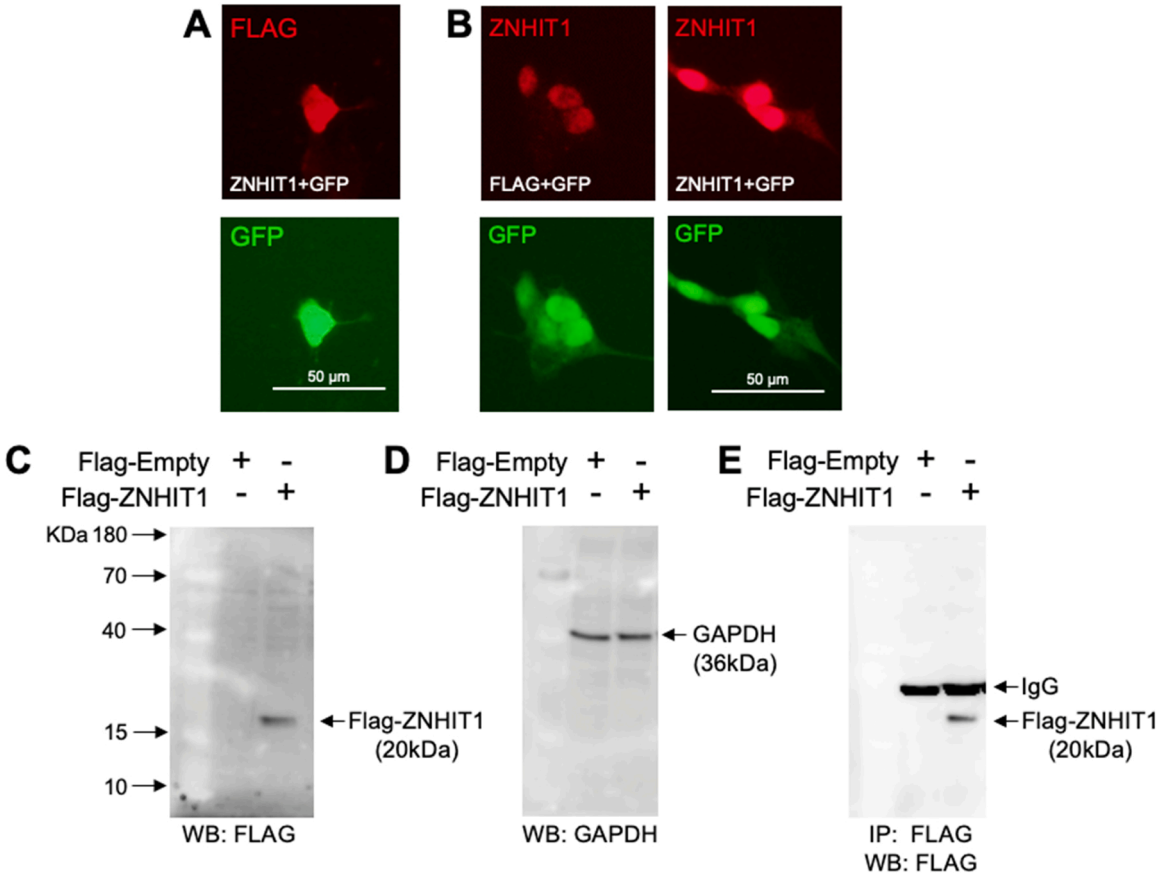

Fig. 2. Immunoprecipitation of FLAG-tagged ZNHIT1 in SH-SY5Y cells.
(A, B) Representative photomicrographs of SH-SY5Y cells transfected with 500 ng of a plasmid expressing either FLAG (Addgene #31,385) or N-terminal FLAG-tagged ZNHIT1 (Addgene #15,332), together with a plasmid expressing GFP, and immunocytochemically stained for (A) FLAG or (B) ZNHIT1, to show co-localisation with GFP at 72 h post-transfection. (C, D) Western blots showing (C) ZNHIT1 or (D) GAPDH expression in SH-SY5Y cells at 24 h after transfection with 2 μg of a plasmid expressing FLAG-ZNHIT1 (Addgene plasmid #15332). (E) Western blotting showing successful pulldown of FLAG-ZNHIT1 using anti-FLAG antibodies at 24 h post-transfection. The full uncropped version of the Western blots are available in supplementary Figure 1.

3.2. Establishment of a FLAG-tagged ZNHIT1 immunoprecipitation assay in SH-SY5Y cells

To identify ZNHIT1 binding partners, we used SH-SY5Y cells which are widely used in the study of molecular signalling pathways of relevance to PD (Xicoy et al., 2017). SH-SY5Y cells were transfected with plasmids expressing either FLAG (as a control) or N-terminal FLAG-tagged ZNHIT1, together with a plasmid expressing GFP to identify the transfected cells. Immunocytochemistry showed the co-localisation of GFP and the FLAG tag, which confirmed co-transfection of GFP with FLAG or N-terminal FLAG-tagged ZNHIT1 (Fig. 2A). In agreement, immunocytochemistry confirmed that GFP+ cells also expressed high levels of ZNHIT1 (Fig. 2B). We next performed Western blotting using protein extracts from cells transfected with either FLAG or FLAG-tagged ZNHIT1 and then carried out an immunoprecipitation using anti-FLAG antibodies. Western blotting for GAPDH confirmed equal protein expression in both groups (Fig. 2C, D), while immunoprecipitation confirmed successful pull-down of FLAG-tagged ZNHIT1 (Fig. 2E). This data confirmed the successful immunoprecipitation of ZNHIT1 from SH-SY5Y cells.

3.3. Proteomics analysis identifies ZNHIT1-interacting proteins that are associated with ATP generation and mitochondrial function

To identify ZNHIT1-interacting proteins, proteins were extracted from the excised gel lanes from the immunoprecipitation and were analysed by label-free mass spectrometry. The resulting peptides were identified using Mascot and Sequest search engines against Uniprot Human Taxonomy databases. An FDR of 1% was used to identify unique peptides mapping to a specific protein. This analysis identified 25 ZNHIT1-interacting proteins (Table 1). We next examined this list of ZNHIT1-interacting proteins to determine if it contained any proteins that might be candidates involved in the regulation of mitochondrial function. The list included mitochondrial proteins such as '*ATP synthase subunit alpha, mitochondrial*' (UniProtKB - P25705) and '*ATP synthase subunit beta, mitochondrial*' (UniProtKB - P06576), which are important for the production of ATP. This suggested the ZNHIT1-interacting proteins may be enriched in those associated with mitochondrial function, therefore we investigated this further using a bioinformatics approach.

Table 1
Proteomics analysis showing the list of ZNHIT1-interacting proteins.

Uniprot ID	Accession	Protein name	Symbol
O43257	ZNHIT1_HUMAN	Zinc finger HIT domain-containing protein 1	ZNHIT1
P62258	1433E_HUMAN	14–3–3 protein epsilon	YWHAE
P27348	1433T_HUMAN	14–3–3 protein theta	YWHAQ
P25705	ATPA_HUMAN	ATP synthase subunit alpha, mitochondrial	ATP5F1A
P06576	ATPB_HUMAN	ATP synthase subunit beta, mitochondrial	ATP5F1B
Q9UQM7	KCC2A_HUMAN	Calcium/calmodulin-dependent protein kinase type II subunit-α	CAMK2A
Q9UBG3	CRNN_HUMAN	Cornulin	CRNN
P14625	ENPL_HUMAN	Endoplasmin	HSP90B1
P02751	FINC_HUMAN	Fibronectin	FN1
O75369	FLNB_HUMAN	Filamin-B	FLNB
P05062	ALDOB_HUMAN	Fructose-biphosphate aldolase B	ALDOB
P17066	HSP76_HUMAN	Heat shock 70 kDa protein 6	HSPA6
P54652	HSP72_HUMAN	Heat shock-related 70 kDa protein 2	HSPA2
A0A075B6P5	KV228_HUMAN	Immunoglobulin kappa variable 2–28	IGKV2–28
A0A087WW87	KV240_HUMAN	Immunoglobulin kappa variable 2–40	IGKV2–40
Q2M215	K1C24_HUMAN	Keratin, type I cytoskeletal 24	KRT24
Q7Z406	MYH14_HUMAN	Myosin-14	MYH14
P41219	PERI_HUMAN	Peripherin	PRPH
P0CG39	POTEJ_HUMAN	POTE ankyrin domain family member J	POTEJ
Q7L014	DDX46_HUMAN	Probable ATP-dependent RNA helicase DDX46	DDX46
A0A075B6R9	KVD24_HUMAN	Probable non-functional immunoglob. k variable 2D-24	IGKV2D-24
Q02383	SEMG2_HUMAN	Semenogelin-2	SEMG2
015020	SPTN2_HUMAN	Spectrin beta chain, non-erthyrocytic 2	SPTBN2
P31629	ZEP2_HUMAN	Transcription factor HIVEP2	HIVEP2
P68366	TBA4A_HUMAN	Tubulin alpha-4A chain	TUBA4A

3.4. Bioinformatics analysis indicates that ZNHIT1-interacting proteins are significantly enriched in proteins associated with mitochondrial function

To investigate this further, we performed a number of enrichment analyses using the Panther classification system (http://pantherdb.org; Version 17.0), to identify functional categories overrepresented in the list of ZNHIT1-interacting proteins. GO enrichment analysis revealed a statistically significant overrepresentation of genes associated with the multiple GO categories associated with mitochondrial function, including '*mitochondrial transport*' (GO: 0006839; FDR = 1.47×10^{-02}), '*mitochondrial proton-transporting ATP synthase, catalytic core*' (GO:0005754; FDR = 2.06×10^{-03}) and '*ATP-dependent activity*' (GO:0140657; FDR = 2.31×10^{-02}) (Table 2). Furthermore, there was a statistically significant overrepresentation of proteins associated with two Panther pathways, ie. '*Parkinson's disease*' (P00049; FDR = 1.39×10^{-03}) and '*ATP synthesis*' (P02721; FDR = 2.92×10^{-03}) (Table 2). We sought to gain further insight by generating a protein–protein interaction (PPI) network using STRING (https://string-db.org), to determine if there were biological relationships among the list of proteins that were found to interact with ZNHIT1. We used an interaction score of 0.4, which is a 'medium confidence' setting. The resultant PPI network generated with the ZNHIT1-interacting proteins had 22 nodes and 18 edges (observed = 18; expected = 6, from a random list of the same size), with a PPI enrichment *p*-value of 7.65×10^{-05} (Fig. 3). This PPI network analysis indicated that ZNHIT1-interacting proteins are biologically connected, and that Heat Shock Protein 90 Beta Family Member 1 (HSP90B1), which is an ATP-metabolising molecular chaperone with roles in stabilising and folding of other proteins (Lackie et al., 2017), may be a potential hub protein. Collectively, these data show that ZNHIT1-interacting proteins are enriched in those regulating ATP production and mitochondrial function and support the suggestion that ZNHIT1 can bind to cytoplasmic proteins that affect mitochondrial function.

3.5. Alterations in co-expression of ZNHIT with the dopaminergic markers TH and ALDH1A1 in the PD SN

Gene co-expression analysis is an bioinformatics approach used to study disease genes of interest (van Dam et al., 2018; Yin et al., 2021), based on the principle that the co-expression patterns of genes that normally have a coordinated pattern of co-expression can be lost in disease states (Torkamani et al., 2010; Zhang et al., 2013; Southworth et al., 2009). We examined the co-expression of *ZNHIT1* with the dopaminergic markers *TH* and *ALDH1A1* in the SN of age- and gender-matched control ($n = 8$) and PD ($n = 15$) samples (GSE49036) (Dijkstra et al., 2015). In control samples, *ZNHIT1* expression was significantly correlated with that of *TH* ($r = 0.874$, $p = 0.0046$) and *ALDH1A1* ($r = 0.740$, $p = 0.036$) (Fig. 4A). In contrast, the correlation of *ZNHIT1* with *TH* ($r = 0.234$, $p = 0.401$) and *ALDH1A1* ($r = 0.290$, $p = 0.295$) was lost in the PD samples (Fig. 4B). To further investigate this, we also stained brain sections control and age-matched PD SN

Table 2
Gene ontology categories that are overrepresented in the list of ZNHIT1-interacting proteins identified in the proteomics analysis.

GObp term ID	GO biological process (GObp)	*n*	+ /-	*p* value	FDR
GO: 0009408	response to heat	4	+	6.62E-06	3.46E-02
GO: 0006839	mitochondrial transport	5	+	1.88E-06	1.47E-02
GO:0006996	organelle organisation	15	+	1.73E-06	2.72E-02
GOcc term ID	**GO cell compartment (GOcc)**	***n***	**+ /-**	***p* value**	**FDR**
GO:0005754	mitochondrial proton-transporting ATP synthase, catalytic core	2	+	9.16E-06	2.06E-03
GO:0045098	type III intermediate filament	2	+	2.29E-05	4.63E-03
GO:0070062	extracellular exosome	17	+	1.83E-11	1.83E-08
GOmf term ID	**GO molecular function (GOmf)**	***n***	**+ /-**	***p* value**	**FDR**
GO:0140657	ATP-dependent activity	7	+	4.72E-06	2.31E-02

Panther pathway ID	Panther pathway name	*n*	+ /-	*p* value	FDR
P00049	Parkinson's disease	7	+	8.71E-06	1.39E-03
P02721	ATP synthesis	2	+	5.48E-05	2.92E-03

samples for ZNHIT1 and TH. While TH+ neurons expressed ZNHIT1 in control brain samples, this was reduced in the PD samples (Fig. 4 C). Therefore the reductions in ZNHIT1 are consistent with impaired ability for ATP generation in the SN in PD, given our previous report showing that ZNHIT1 overexpression increases ATP production (McCarthy et al., 2022).

4. Discussion

We have previously shown that ZNHIT1 overexpression was sufficient to prevent α-synuclein-mediated dysregulation of mitochondrial respiration and neurite growth, and to increase cellular ATP (McCarthy et al., 2022). This provided proof for a functional role of ZNHIT1 in neuronal growth and in the regulation of cellular bioenergetic state, and suggested that ZNHIT1 may be a therapeutic target for PD. However there is limited information about ZNHIT1 expression in the human brain and it is important to investigate this. Here we show that ZNHIT1 is expressed in multiple brain regions, with the highest level of expression in the SN. In agreement, semiquantitative RT-PCR analysis of human tissue has previously shown that the highest levels of ZNHIT1 expression are in the foetal and adult brain, followed by the kidney, heart and spleen (Cuadrado et al., 2007). Further analysis in our study revealed that ZNHIT1 expression is strongest in neurons and is primarily concentrated in the nucleus but is also present in the cytoplasm. This agrees with a previous study showing perinuclear distribution of ZNHIT1 in the nucleus of transfected Hela and HepG2 cancer cells (Wang et al., 2007). Furthermore, endogenous ZNHIT1 has been shown to localise to the nucleus in mouse embryonic fibroblasts (Cuadrado et al., 2007). This is consistent with data showing that ZNHIT1 functions within the nucleosome as a core component of the SRCAP chromatin-remodelling complex to mediate H2A.Z exchange in the regulation of transcriptional activation in mouse (Cuadrado et al., 2010) and neuronal cellular models (McCarthy et al., 2022). Collectively, these data show that ZNHIT1 is expressed in the nucleus of neurons but also

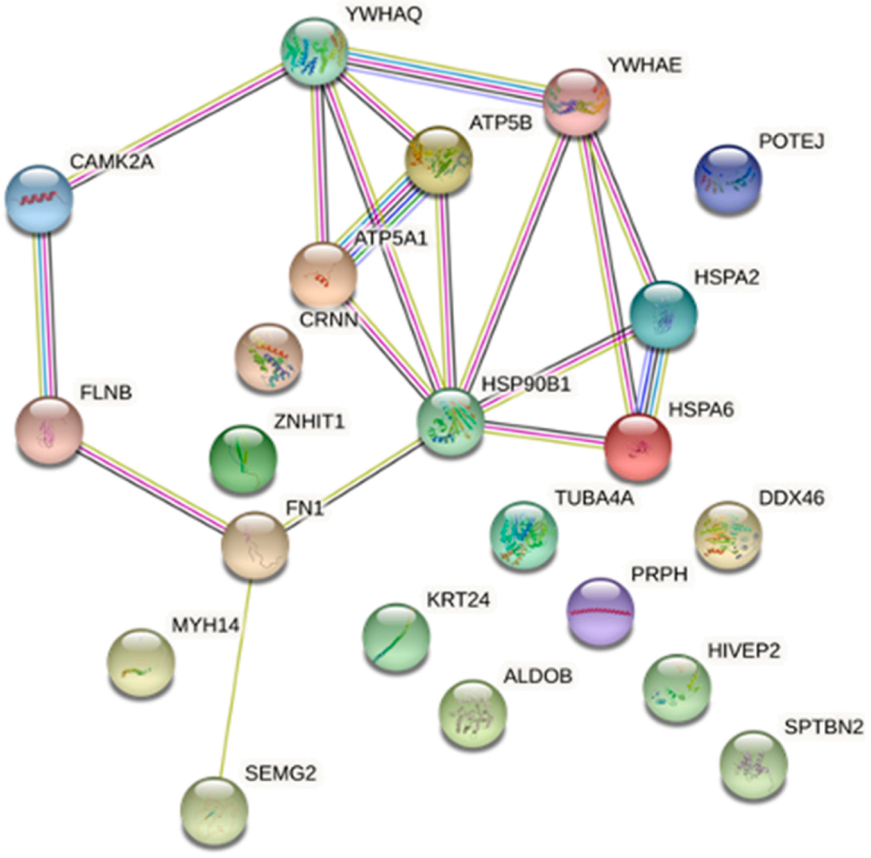

Fig. 3. Protein-protein interaction network analysis indicates that ZNHIT1-interacting proteins are biologically connected as a group. This protein–protein interaction (PPI) network was generated from the list of ZNHIT1-interacting proteins, using the STRING platform (https://string-db.org).

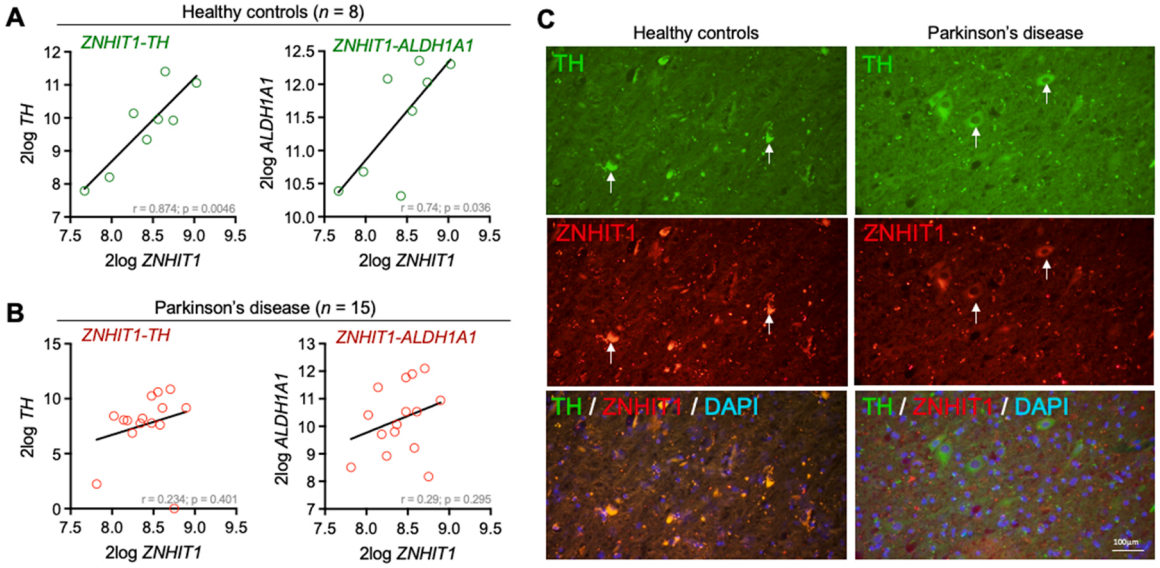

Fig. 4. Alterations in co-expression of *ZNHIT* with the dopaminergic markers *TH* and *ALDH1A1* in the PD SN. Raw data were derived from dataset GSE49036, and the R2 microarray platform was used to analyse the co-expression of *ZNHIT1* in control and PD samples. (A, B) Linear regression analysis showing correlations between *ZNHIT1* and *TH* or *ALDH1A1* in (A) Control *(n = 8)* and (B) PD samples. The *r* and associated p values are shown on each graph. (C) Representative photomicrographs of TH and ZNHIT1 immunostaining (white arrows) in the SN in post-mortem sections of control and PD human brains. Scale bar = 100 μm.

that ZNHIT1 is expressed, albeit at lower levels, in the cytoplasm, indicating that ZNHIT1 may also function outside of the nucleus.

To investigate this further, we identified potential interacting partners of ZNHIT1. Our analysis identified 25 ZNHIT1-interacting proteins. Having obtained this list of proteins, we next performed a GO enrichment analysis to identify any significant functional enrichments in this interactome. This revealed that the ZNHIT1-interacting proteins were involved in mitochondrial transport, mitochondrial protein transporting ATP synthesis, ATP synthesis and in pathways associated with PD. These findings agree with our previous data showing that ZNHIT1 regulates ATP synthesis in SH-SY5Y cells (McCarthy et al., 2022). In support of this, other studies have revealed a regulatory role for ZNHIT1 in gene expression associated with mitochondrial function during prenatal heart development (Xu et al., 2021b). Moreover, ZNHIT1 knockout (*KO-ZNHIT1*) mice show reduced ATP synthesis as a consequence of reduced embryonic expression of several mitochondrial proteins in cardiac myocytes (Xu et al., 2021b). Although that study reported reductions in the expression of several mitochondrial proteins, here we found that ZNHIT1 protein interacts with ATP-synthase5A1 and ATP5B. This protein-protein interaction could provide a mechanism for extracellular-mitochondrial roles of ZNHIT1. Both ATP5A1 and ATP5B form an integral part of mitochondrial ATP synthesis complex V (Jonckheere et al., 2012). Thus if ZNHIT1 protein interacts with mitochondrial complex V, it could play a regulatory role in mitochondria. The mitochondrial complex V (consisting of ATPA1A and ATPB5) and its interaction with ZNHIT1 could be crucial for ATP synthesis, since complex V is the ATP-synthesising machinery (Jonckheere et al., 2012; Hamacher-Brady and Brady, 2016). This is consistent with our previous study which reported increased ATP synthesis as a consequence of ZNHIT1 overexpression (McCarthy et al., 2022), as well as with the study by Xu and colleagues showing a decrease in ATP synthesis due to ZNHIT1 knockout (Xu et al., 2021b). Collectively, these data suggest that ZNHIT1 protein may play an extranuclear-mitochondrial role in regulating mitochondrial complex V and ATP synthesis.

In support of this, our study also identified several other interacting partners of ZNHIT1, which regulate mitochondrial respiration. Furthermore, our STRING PPI analysis revealed HSP90B1 as a potential hub protein. Interestingly, a link to PD comes from a study showing that transcripts for HSP90B1 mRNA levels are upregulated in post-mortem brain sections from patients with PD or dementia with Lewy bodies (Bohush et al., 2019). That study also found that HSP90B transcripts were upregulated in Lewy-positive neurons in frontal and temporal cortex of PD brains, and in the Lewy-positive neurons in the SN of dementia with Lewy bodies brains, and the authors suggest a potential neuroprotective role for HSP90B1 in these diseases (Bohush et al., 2019). Huang et al. reported an increase in HSP90B1 expression in MN9D dopaminergic cells that had been exposed to the neurotoxin MPP^+ (Huang et al., 2013). In addition, silencing of regulated endocrine specific protein 18 (RESP18), which is a negative regulator of HSP90B1, reduced cell death in MPP+-treated MN9D cells, through the upregulation of HSP90B1 (Huang et al., 2013). HSP90B1 is known to prevent α-synuclein aggregation and to deter pathological progression in SH-SY5Y models of PD, by increasing the solubility of α-synuclein oligomers (Daturpalli et al., 2013). Furthermore, HSP90B1 is a known interacting partner of Leucine rich repeat kinase (LRRK)2 (Ko et al., 2009), and in the LKRR2 G2019S midbrain organoid model of PD, HSP90B1 protein levels were significantly reduced (Zagare et al., 2022). In addition, HSP90B1 levels have been found to be upregulated following treatment of PD patient-derived fibroblast cells with the anti-oxidant, resveratrol (Vergara et al., 2017).

In our study, we assessed the expression of HSP90B1 in human brain and found that in normal post-mortem SN samples, HSP90B1 mRNA, like that of ZNHIT1, was highest in the SN. Their co-expression in these brain regions hints at a possible functional association between ZNHIT1 and HSB90B1 in vivo, which potentially puts their interaction into context in the human SN. Since the expression of ZNHIT1 restores mitochondrial functioning in cellular models of PD (McCarthy et al., 2022), and expression of HSP90B1 deters the progression of PD pathology by enhancing the solubility of α-synuclein oligomers, this presents a potential role for dysfunction of ZNHIT1 and HSP90B1 in the molecular pathology involved in PD (Daturpalli et al., 2013). To study this further, we investigated whether the gene co-expression patterns of *ZNHIT1* and the dopaminergic markers *TH* and *ALDH1A1* were altered in the SN of control and PD samples. The rational was that co-expression patterns break down in disease states, and such broken correlations can indicate functional misregulation (Torkamani et al., 2010; Zhang et al., 2013; Southworth et al., 2009). Our gene co-expression analysis revealed a significant correlation between *ZNHIT1* and both *TH* and *ALDH1A1* in control samples, and this correlation was lost in PD. This is suggestive of a functional dysregulation of ZNHIT1 in PD.

In summary, ZNHIT1 has been shown to promote mitochondrial function and ATP production (McCarthy et al., 2022; Xu et al., 2021b). Here we build on these reports by performing a combined proteomics and bioinformatics analysis, which revealed that ZNHIT1-interacting proteins are significantly enriched in those associated with mitochondrial function and ATP synthesis. This is consistent with previous studies indicating a neuroprotective role for ZNHIT1 against α-synuclein-induced mitochondrial dysfunction in PD (McCarthy et al., 2022). Our results suggest that ZNHIT1 may mediate its neuroprotective effects through an interaction with mitochondrial proteins in the cytosol of dopaminergic neurons in the SN. Our gene co-expression studies suggest a functional misregulation of ZNHIT1 in PD, which may result in functional misregulation of its mitochondrial interacting proteins in the cytoplasm, leading to mitochondrial dysfunction that is typically seen in PD. These findings rationalise the continued study of the nuclear and extra-nuclear effects of ZNHIT1 in the regulation of mitochondrial function, in the context of development of neuroprotective therapies for PD.

Author contributions

JA carried out the immunoprecipitation and coordinated the proteomics analysis. EM, JA and GOK performed the bioinformatics analysis. JA and EM carried out cell culture experiments. EM and GOK interrogated the Human Protein Atlas. FW and MM performed the immunohistochemistry. JA, EM, FW, AS and GOK analysed data, prepared figures and wrote manuscript. All authors edited the final manuscript. NMP, MM, LC, AS & GOK designed the study and supervised the work.

Funding

This publication has emanated from research conducted with the financial support of Science Foundation Ireland (SFI) under grant number 19/FFP/6666 (G.O'K.), the Irish Research Council (GOIPG-2018-2795; E.Mc/2022/A.S./G.O'K), the Marie Skłodowska-Curie Fellowship programme under grant number MSCA-IF-2019 890290 (N. M.P/A.S./G.O'K), and Cure Parkinson's under grant number CP:GO01 (A.S./G.O'K).

Ethical statement

As this work used commercially human cell lines or open-source repositories of human brain data, no ethical approval for any of those experiments. For immunohistochemistry on human brain samples, brain section were supplied under full ethical approval by the Parkinson's UK Brain Bank at Imperial College London, funded by Parkinson's UK, a charity registered in England and Wales (258197) and in Scotland (SC037554).

CRediT authorship contribution statement

Jayanth Anantha: Conceptualization, Methodology, Formal analysis, Writing – original draft. **Fionnuala E. Wilson:** Conceptualization, Methodology, Formal analysis, Writing – original draft. **Erin McCarthy:** Formal analysis, Writing – review & editing. **Noelia Morales Prieto:** Supervision, Methodology, Writing – review & editing. **Martina Mazzocchi:** Supervision, Methodology, Writing – review & editing. **Louise M. Collins:** Supervision, Funding acquisition, Writing – review & editing. **Aideen M. Sullivan:** Supervision, Funding acquisition, Conceptualization, Writing - original draft. **Gerard W. O'Keeffe:** Conceptualization, Supervision, Funding acquisition, Formal analysis, Writing – original draft.

Declaration of Competing Interest

The authors declare that the research was conducted in the absence of any commercial or financial relationships that could be construed as a potential conflict of interest.

Data Availability

Data will be made available on request.

Appendix A. Supporting information

Supplementary data associated with this article can be found in the online version at doi:10.1016/j.jchemneu.2023.102288.

References

Khakh, B.S., Burnstock, G., 2009. The double life of ATP. Sci. Am. 301 (84–90), 92.
Pathak, D., Shields, L.Y., Mendelsohn, B.A., Haddad, D., Lin, W., Gerencser, A.A., Kim, H., Brand, M.D., Edwards, R.H., Nakamura, K., 2015. The role of mitochondrially derived ATP in synaptic vesicle recycling. J. Biol. Chem. 290, 22325–22336.
Blaszczyk, J.W., 2020. Energy metabolism decline in the aging brain-pathogenesis of neurodegenerative disorders. Metabolites 10.
Li, J.L., Lin, T.Y., Chen, P.L., Guo, T.N., Huang, S.Y., Chen, C.H., Lin, C.H., Chan, C.C., 2021. Mitochondrial function and Parkinson's disease: from the perspective of the electron transport chain. Front Mol. Neurosci. 14, 797833.
Moon, H.E., Paek, S.H., 2015. Mitochondrial dysfunction in Parkinson's disease. Exp. Neurobiol. 24, 103–116.
Bloem, B.R., Okun, M.S., Klein, C., 2021. Parkinson's disease. Lancet 397, 2284–2303.
Goedert, M., Compston, A., 2018. Parkinson's disease - the story of an eponym. Nat. Rev. Neurol. 14, 57–62.
Kordower, J.H., Olanow, C.W., Dodiya, H.B., Chu, Y., Beach, T.G., Adler, C.H., Halliday, G.M., Bartus, R.T., 2013. Disease duration and the integrity of the nigrostriatal system in Parkinson's disease. Brain 136, 2419–2431.
Spillantini, M.G., Crowther, R.A., Jakes, R., Hasegawa, M., Goedert, M., 1998. alpha-Synuclein in filamentous inclusions of Lewy bodies from Parkinson's disease and dementia with lewy bodies. Proc. Natl. Acad. Sci. USA 95, 6469–6473.
Spillantini, M.G., Schmidt, M.L., Lee, V.M., Trojanowski, J.Q., Jakes, R., Goedert, M., 1997. Alpha-synuclein in Lewy bodies. Nature 388, 839–840.
Park, J.H., Burgess, J.D., Faroqi, A.H., DeMeo, N.N., Fiesel, F.C., Springer, W., Delenclos, M., McLean, P.J., 2020. Alpha-synuclein-induced mitochondrial dysfunction is mediated via a sirtuin 3-dependent pathway. Mol. Neurodegener. 15, 5.
Wang, X., Becker, K., Levine, N., Zhang, M., Lieberman, A.P., Moore, D.J., Ma, J., 2019. Pathogenic alpha-synuclein aggregates preferentially bind to mitochondria and affect cellular respiration. Acta Neuropathol. Commun. 7, 41.
Nakano, M., Imamura, H., Sasaoka, N., Yamamoto, M., Uemura, N., Shudo, T., Fuchigami, T., Takahashi, R., Kakizuka, A., 2017. ATP maintenance via two types of ATP regulators mitigates pathological phenotypes in mouse models of Parkinson's Disease. EBioMedicine 22, 225–241.
Cai, R., Zhang, Y., Simmering, J.E., Schultz, J.L., Li, Y., Fernandez-Carasa, I., Consiglio, A., Raya, A., Polgreen, P.M., Narayanan, N.S., Yuan, Y., Chen, Z., Su, W., Han, Y., Zhao, C., Gao, L., Ji, X., Welsh, M.J., Liu, L., 2019. Enhancing glycolysis attenuates Parkinson's disease progression in models and clinical databases. J. Clin. Invest 129, 4539–4549.
Morrison, A.J., Shen, X., 2009. Chromatin remodelling beyond transcription: the INO80 and SWR1 complexes. Nat. Rev. Mol. Cell Biol. 10, 373–384.
Lowden, C., Boulet, A., Boehler, N.A., Seecharran, S., Rios Garcia, J., Lowe, N.J., Liu, J., Ong, J.L.K., Wang, W., Ma, L., Cheng, A.H., Senatore, A., Monks, D.A., Liu, B.H., Leary, S.C., Cheng, H.M., 2021. Homeostatic control of nuclear-encoded mitochondrial gene expression by the histone variant H2A.Z is essential for neuronal survival. Cell Rep. 36, 109704.
McCarthy, E., Barron, A., Morales-Prieto, N., Mazzocchi, M., McCarthy, C.M., Collins, L. M., Sullivan, A.M., O'Keeffe, G.W., 2022. Gene Co-expression analysis of the human substantia nigra identifies ZNHIT1 as an SNCA co-expressed gene that protects against alpha-synuclein-induced impairments in neurite growth and mitochondrial dysfunction in SH-SY5Y cells. Mol. Neurobiol.
Xu, M., Yao, J., Shi, Y., Yi, H., Zhao, W., Lin, X., Yang, Z., 2021a. The SRCAP chromatin remodeling complex promotes oxidative metabolism during prenatal heart development. Development 148.
Lindenboim, L., Borner, C., Stein, R., 2011. Nuclear proteins acting on mitochondria. Biochim Biophys. Acta 1813, 584–596.
Ramasamy, A., Trabzuni, D., Guelfi, S., Varghese, V., Smith, C., Walker, R., De, T., Coin, L., De Silva, R., Cookson, M.R., 2014a. Genetic variability in the regulation of gene expression in ten regions of the human brain. Nat. Neurosci. 17, 1418–1428.
Dijkstra, A.A., Ingrassia, A., de Menezes, R.X., van Kesteren, R.E., Rozemuller, A.J., Heutink, P., van de Berg, W.D., 2015. Evidence for immune response, axonal dysfunction and reduced endocytosis in the substantia nigra in early stage Parkinson's disease. PLoS One 10, e0128651.
Uhlen, M., Fagerberg, L., Hallstrom, B.M., Lindskog, C., Oksvold, P., Mardinoglu, A., Sivertsson, A., Kampf, C., Sjostedt, E., Asplund, A., Olsson, I., Edlund, K., Lundberg, E., Navani, S., Szigyarto, C.A., Odeberg, J., Djureinovic, D., Takanen, J.O., Hober, S., Alm, T., Edqvist, P.H., Berling, H., Tegel, H., Mulder, J., Rockberg, J., Nilsson, P., Schwenk, J.M., Hamsten, M., von Feilitzen, K., Forsberg, M., Persson, L.,

Johansson, F., Zwahlen, M., von Heijne, G., Nielsen, J., Ponten, F., 2015. . Proteom. Tissue-Based map Hum. Proteome Sci. 347, 1260419.
Ramasamy, A., Trabzuni, D., Guelfi, S., Varghese, V., Smith, C., Walker, R., De, T., Consortium, U.K.B.E., North American Brain Expression, C., Coin, L., de Silva, R., Cookson, M.R., Singleton, A.B., Hardy, J., Ryten, M., Weale, M.E., 2014b. Genetic variability in the regulation of gene expression in ten regions of the human brain. Nat. Neurosci. 17, 1418–1428.
Xicoy, H., Wieringa, B., Martens, G.J., 2017. The SH-SY5Y cell line in Parkinson's disease research: a systematic review. Mol. Neurodegener. 12, 10.
Lackie, R.E., Maciejewski, A., Ostapchenko, V.G., Marques-Lopes, J., Choy, W.Y., Duennwald, M.L., Prado, V.F., Prado, M.A.M., 2017. The Hsp70/Hsp90 chaperone machinery in neurodegenerative diseases. Front Neurosci. 11, 254.
van Dam, S., Vosa, U., van der Graaf, A., Franke, L., de Magalhaes, J.P., 2018. Gene co-expression analysis for functional classification and gene-disease predictions. Brief. Bioinform 19, 575–592.
Yin, W., Mendoza, L., Monzon-Sandoval, J., Urrutia, A.O., Gutierrez, H., 2021. Emergence of co-expression in gene regulatory networks. PLoS One 16, e0247671.
Torkamani, A., Dean, B., Schork, N.J., Thomas, E.A., 2010. Coexpression network analysis of neural tissue reveals perturbations in developmental processes in schizophrenia. Genome Res. 20, 403–412.
Zhang, B., Gaiteri, C., Bodea, L.-G., Wang, Z., McElwee, J., Podtelezhnikov, A.A., Zhang, C., Xie, T., Tran, L., Dobrin, R., 2013. Integrated systems approach identifies genetic nodes and networks in late-onset Alzheimer's disease. Cell 153, 707–720.
Southworth, L.K., Owen, A.B., Kim, S.K., 2009. Aging mice show a decreasing correlation of gene expression within genetic modules. PLoS Genet. 5, e1000776.
Cuadrado, A., Lafarga, V., Cheung, P.C., Dolado, I., Llanos, S., Cohen, P., Nebreda, A.R., 2007. A new p38 MAP kinase-regulated transcriptional coactivator that stimulates p53–dependent apoptosis. EMBO J. 26, 2115–2126.
Wang, J., Li, Y., Zhang, M., Liu, Z., Wu, C., Yuan, H., Li, Y.Y., Zhao, X., Lu, H., 2007. A zinc finger HIT domain-containing protein, ZNHIT-1, interacts with orphan nuclear hormone receptor Rev-erbβ and removes Rev-erbβ-induced inhibition of apoCIII transcription. The. FEBS J. 274, 5370–5381.
Cuadrado, A., Corrado, N., Perdiguero, E., Lafarga, V., Muñoz-Canoves, P., Nebreda, A. R., 2010. Essential role of p18Hamlet/SRCAP-mediated histone H2A. Z chromatin incorporation in muscle differentiation. The. EMBO J. 29, 2014–2025.
Xu, M., Yao, J., Shi, Y., Yi, H., Zhao, W., Lin, X., Yang, Z., 2021b. The SRCAP chromatin remodeling complex promotes oxidative metabolism during prenatal heart development. Dev. 148, dev1 99026.
Jonckheere, A.I., Smeitink, J.A., Rodenburg, R.J., 2012. Mitochondrial ATP synthase: architecture, function and pathology. J. Inherit. Metab. Dis. 35, 211–225.
Hamacher-Brady, A., Brady, N.R., 2016. Mitophagy programs: mechanisms and physiological implications of mitochondrial targeting by autophagy. Cell. Mol. Life Sci. 73, 775–795.
Bohush, A., Niewiadomska, G., Weis, S., Filipek, A., 2019. HSP90 and Its Novel Co-Chaperones, SGT1 and CHP-1, in brain of patients with Parkinson's disease and dementia with Lewy Bodies. J. Park. Dis. 9, 97–107.
Huang, Y., Xu, J., Liang, M., Hong, X., Suo, H., Liu, J., Yu, M., Huang, F., 2013. RESP18 is involved in the cytotoxicity of dopaminergic neurotoxins in MN9D cells. Neurotox. Res 24, 164–175.
Daturpalli, S., Waudby, C.A., Meehan, S., Jackson, S.E., 2013. Hsp90 inhibits α-synuclein aggregation by interacting with soluble oligomers. J. Mol. Biol. 425, 4614–4628.
Ko, H.S., Bailey, R., Smith, W.W., Liu, Z., Shin, J.-H., Lee, Y.-I., Zhang, Y.-J., Jiang, H., Ross, C.A., Moore, D.J., Patterson, C., Petrucelli, L., Dawson, T.M., Dawson, V.L., 2009. CHIP regulates leucine-rich repeat kinase-2 ubiquitination, degradation, and toxicity. Proc. Natl. Acad. Sci. USA 106, 2897–2902.
Zagare, A., Barmpa, K., Smajic, S., Smits, L.M., Grzyb, K., Grünewald, A., Skupin, A., Nickels, S.L., Schwamborn, J.C., 2022. Midbrain organoids mimic early embryonic neurodevelopment and recapitulate LRRK2-p.Gly2019Ser-associated gene expression. Am. J. Hum. Genet. 109, 311–327.
Vergara, D., Gaballo, A., Signorile, A., Ferretta, A., Tanzarella, P., Pacelli, C., Di Paola, M., Cocco, T., Maffia, M., 2017. Resveratrol Modul. Protein Expr. Park. -Mutant Hum. Ski. Fibroblasts: A Prote Approach Oxid. Med. Cell. Longev. 2017, 2198243.